

Light propagation in a random three-dimensional ensemble of point scatterers in a waveguide: Size-dependent switching between diffuse radiation transfer and Anderson localization of light

A. S. Kuraptsev^{✉*} and I. M. Sokolov^{✉†}*Peter the Great St. Petersburg Polytechnic University, 195251, St. Petersburg, Russia*

(Received 6 February 2022; accepted 19 May 2022; published 21 June 2022)

Light transport in a disordered ensemble of resonant atoms placed in a waveguide is found to be very sensitive to the sizes of the cross section of a waveguide. Based on a self-consistent quantum microscopic model treating atoms as coherent radiating dipoles, we have shown that the nature of radiation transfer changes from Anderson localization regime in a single-mode waveguide to a traditional diffuse transfer in a multimode one. Moreover, the transmittance magnitude undergoes complicated steplike nonmonotonic dependence on the transverse sizes of a waveguide.

DOI: [10.1103/PhysRevA.105.063513](https://doi.org/10.1103/PhysRevA.105.063513)

I. INTRODUCTION

The transition from extended to localized eigenstates upon increasing disorder in a quantum or wave system is named after Philip Anderson who was the first to predict it for electrons in disordered solids [1]. This transition manifests itself in sharp decrease of the diffusion coefficient for electrons down to zero and associated suppression of the conductivity, thus a conducting medium turns into a dielectric. Actually, the effect of phase transition induced by disorder has a general nature. More recently, it was studied for various types of quantum particles (cold atoms [2], Bose-Einstein condensates [3]) as well as for classical waves (light [4–6], ultrasound [7,8]). Anderson localization of light may find applications in the design of future quantum-information devices [9], miniature lasers [10], and solar cells [11]. Drawing a parallel between Anderson localization predicted for electrons in solids and localization of light in a dispersive medium, the analog of the metallic phase is the regime of diffuse radiation transfer whereas the analog of nonconducting phase is represented in the Anderson localization of light. The phenomenon of Anderson localization of light can manifest itself in various physical systems, but special attention is paid to random ensembles of point scatterers (such as cold atomic gases or impurity atoms embedded in a solid transparent dielectric matrix). This is connected with the fact that these objects represent an excellent playground for testing the theory.

In the literature, one can find different signs for Anderson localization of light based on eigenstates diagram (mainly, lifetimes of eigenstates), on the character of radiation trapping, on the inverse participation ratio, on the Ioffe-Regel parameter, on the Thouless number, to name a few. However, these signs represent the necessary conditions for Anderson localization but are not sufficient ones. The most reliable criterion comes from the exact definition of localization, namely the transmittance in a stationary mode must exponentially decrease with increasing of the thickness of a sample. There

are also some requirements, which have to be met if we want to use this criterion. The first is the absence of any relaxation channels which lead to energy losses of the joint atomic-field system. This circumstance is not a problem in theoretical simulations, but it can represent a critical point for experiments since the existence of such channels permits alternative explanations for exponential behavior of the transmittance [12–14]. The second is that a medium has to be optically dense, so the intensity of transmitted light is determined mainly by its incoherent component. Actually, both these requirements are valid not only in the case of transmission criterion but also for all other signs for Anderson localization of light.

By now, it has been understood that Anderson localization of light in a random three-dimensional (3D) ensemble of point scatterers without applying external control fields is absent [15]. However, a static magnetic field restores Anderson localization of light in a cold-atom gas [16]. The situation essentially changes when we deal with low-dimensional systems [17]. It is known that in two dimensions, there is no true metallic behavior of a disordered electronic system [18]. Thus, reduced dimensionality facilitates the achievement of Anderson localization. This also holds true when understanding Anderson localization in a broad sense, including both metal-insulator transitions and quantum-Hall-type transitions between phases with localized states [19]. Focusing on the Anderson localization of light in atomic ensembles, it is worth to note that the fabrication of low-dimensional ensembles usually assumes their coupling with a cavity or waveguide structures [20,21]. This imprints the nature of interaction between atoms and electromagnetic field, that, in turn, leads to a modification of interatomic dipole-dipole interaction [22–24] and associated cooperative effects [25–31]. A correct description of these effects requires a realistic three-dimensional picture both because of 3D arrangement of atoms and, which is more fundamental, because of the vector nature of electromagnetic field. Moreover, we have recently shown that polarization effects play a crucial role in spontaneous decay of an excited atom in a single-mode waveguide [32].

In this paper we report the results of fully 3D calculation of light intensity transmitted through a random ensemble of point scatterers in a waveguide. We show that the nature of

*aleksej-kurapcev@yandex.ru

†ims@is12093.spb.edu

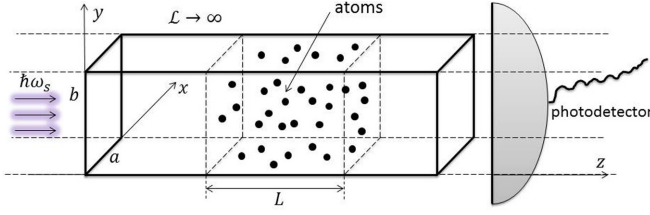


FIG. 1. Sketch of the waveguide and the atomic ensemble inside it.

light transport dramatically depends on the transverse sizes of a waveguide. Thus, when a waveguide is single-mode with respect to resonant transition wavelength, the regime of Anderson localization is realized even for an arbitrarily low atomic density. An increase in the transverse size turns a single-mode waveguide to a multimode one, that, in turn, instantly cancels Anderson localization and restores classical diffuse radiation transfer.

II. BASIC ASSUMPTIONS AND APPROACH

We consider an ensemble of $N \gg 1$ identical two-level atoms at random position $\{\mathbf{r}_i\}$ inside a waveguide, see Fig. 1. The resonant frequency ω_0 of atoms defines the natural length scale $1/k_0 = c/\omega_0$, where c is the vacuum speed of light. The ground state $|g_i\rangle$ of an isolated atom i is nondegenerate with the total angular momentum $J_g = 0$, whereas the excited states $|e_i\rangle$ is threefold degenerate with $J_e = 1$ and natural free space linewidth γ_0 . The three degenerate substates $|e_{i,m_j}\rangle$ correspond to the three possible projections $m_j = 0, \pm 1$ of the total angular momentum \mathbf{J}_e on the quantization axis z . For convenience, let us choose the z axis coinciding with the axis of a waveguide.

The cross section of the waveguide is assumed to be rectangular having the sizes a and b . Atomic ensemble occupies a whole cross section of a waveguide and has the longitudinal length L along the z axis. Both input and output of a waveguide are far remote from the edges of the atomic medium (corresponding separations are much larger than L). Atomic ensemble is illuminated by stationary probe radiation, which is considered to be monochromatic with the frequency ω_s . Transmitted radiation is measured by a photodetector, which absorbs the whole output signal integrated over the area of cross section indifferent to the polarization state.

To describe the stationary regime of atomic excitation induced by external radiation within the framework of consistent quantum-mechanical treatment, we use the following technique. Let us suppose that probe radiation is created as a result of spontaneous emission of some remote atom in a waveguide, which has the same level structure as atoms from an ensemble but different resonance transition frequency ω_s and narrow linewidth γ_s (hereafter we call it the ‘‘source atom’’). It allows us to consider the following initial conditions: only the source atom is excited whereas all other atoms forming an ensemble are in their ground state; the electromagnetic field is in the vacuum state at $t = 0$. Thus, the problem considered here can be formally reduced to the problem of collective spontaneous decay in a waveguide, which we studied previously [32].

Assuming the walls of a waveguide to be perfectly conductive (i.e., neglecting the absorption), the dynamics of the atomic-field system can be treated on the basis of the non-steady-state Schrodinger equation with the following Hamiltonian [33]:

$$\begin{aligned} \hat{H} = & \sum_{i=1}^{N+1} \sum_{m_j=-1}^1 \hbar\omega_0 |e_{i,m_j}\rangle \langle e_{i,m_j}| \\ & + \sum_{\mathbf{k},\alpha} \hbar\omega_k \left(\hat{a}_{\mathbf{k},\alpha}^\dagger \hat{a}_{\mathbf{k},\alpha} + \frac{1}{2} \right) - \sum_{i=1}^{N+1} \hat{\mathbf{d}}_i \cdot \hat{\mathbf{E}}(\mathbf{r}_i) \\ & + \frac{1}{2\epsilon_0} \sum_{i \neq j}^{N+1} \hat{\mathbf{d}}_i \cdot \hat{\mathbf{d}}_j \delta(\mathbf{r}_i - \mathbf{r}_j), \end{aligned} \quad (1)$$

where the first two terms correspond to noninteracting atoms and the electromagnetic field in an empty waveguide, respectively, the third term describes the interaction between the atoms and the field in the dipole approximation, and the last, contact term ensures the correct description of the electromagnetic field radiated by the atoms [33]. In Eq. (1), $\hat{a}_{\mathbf{k},\alpha}^\dagger$ and $\hat{a}_{\mathbf{k},\alpha}$ are the operators of creation and annihilation of a photon in the corresponding mode, ω_k is the photon frequency, $\hat{\mathbf{d}}_i$ is the dipole operator of the atom i , $\hat{\mathbf{E}}(\mathbf{r})$ is the electric displacement vector in a waveguide, and \mathbf{r}_i is the position of the atom i . The vacuum reservoir is also included in the atomic-field system described by the Hamiltonian represented in Eq. (1).

The field operator $\hat{\mathbf{E}}(\mathbf{r})$ can be obtained on the basis of well known classical mode expansion of the electromagnetic field in a waveguide with corresponding boundary conditions [34] followed by standard quantization [35]. The specific form of this operator is determined by the cross section of a waveguide. For the given geometry, $\hat{\mathbf{E}}(\mathbf{r})$ can be read as follows:

$$\begin{aligned} \hat{\mathbf{E}}(\mathbf{r}) = & \sum_{\mathbf{k},\alpha} \sqrt{\frac{\hbar}{2\omega_k}} \mathbf{E}_{\mathbf{k},\alpha}(x, y) \\ & \times \exp(ik_z z) \hat{a}_{\mathbf{k},\alpha} + \text{H.c.}, \end{aligned} \quad (2)$$

where α denotes the type of waveguide mode – TE (transverse electric) or TM (transverse magnetic), i means imaginary unit.

$$E_{\mathbf{k},TE}^x(x, y) = -\frac{ik_n k}{k_m^2 + k_n^2} B_{mn} \cos(k_m x) \sin(k_n y), \quad (3)$$

$$E_{\mathbf{k},TE}^y(x, y) = \frac{ik_m k}{k_m^2 + k_n^2} B_{mn} \sin(k_m x) \cos(k_n y), \quad (4)$$

$$E_{\mathbf{k},TE}^z(x, y) \equiv 0, \quad (5)$$

$$E_{\mathbf{k},TM}^x(x, y) = \frac{ik_z k_m}{k_m^2 + k_n^2} B_{mn} \cos(k_m x) \sin(k_n y), \quad (6)$$

$$E_{\mathbf{k},TM}^y(x, y) = \frac{ik_z k_n}{k_m^2 + k_n^2} B_{mn} \sin(k_m x) \cos(k_n y), \quad (7)$$

$$E_{\mathbf{k},TM}^z(x, y) = B_{mn} \sin(k_m x) \sin(k_n y). \quad (8)$$

Here $k_m = m\pi/a$, $k_n = n\pi/b$, $k = \sqrt{k_m^2 + k_n^2 + k_z^2} = \omega_k/c$. The indexes m and n are positive integers for TM modes, and for TE modes $m, n = 0, 1, 2, \dots$, herewith both indexes

cannot be zero together. B_{mm} is the normalization constant, which can be obtained on the basis of the standard form of the field Hamiltonian. Reference point is chosen at one of the corners of the cross section, so the space into a waveguide corresponds to the positive values of the coordinates x and y , as shown in Fig. 1.

Formally solving the Schrodinger equation for the joint system, which consists of $N + 1$ atom (N atoms of an ensemble + source-atom) and the electromagnetic field, and restricting ourselves by the states containing no more than one photon (i.e., neglecting nonlinear effects), one obtains a system of equations for the amplitudes b_e of one-fold atomic excited states with the coupling between atoms caused by the dipole-dipole interaction. For Fourier components $b_e(\omega)$ we have (at greater length see Ref. [36])

$$\sum_{e'} [(\omega - \omega_e)\delta_{ee'} - \Sigma_{ee'}(\omega)] b_{e'}(\omega) = i\delta_{es}. \quad (9)$$

The index s as well as the indexes e and e' contain information both about the number of atom and about specific atomic sublevel excited in the corresponding state.

The matrix $\Sigma_{ee'}(\omega)$ describes both spontaneous decay and photon exchange between the atoms. It is connected with the Green's matrix $G_{ee'}(\omega)$ by a simple relation $\Sigma_{ee'}(\omega) = (-\gamma_0/2)G_{ee'}(\omega)$.

According to the general quantum microscopic approach essentially based on the coupled-dipole model, the Green's matrix $G_{ee'}(\omega)$ is given as follows:

$$G_{ee'}(\omega) = -\frac{2}{\gamma_0} \left\{ \sum_g V_{e;g} V_{g,e'} \zeta(\hbar\omega - E_g) + \sum_{ee'} V_{e;ee'} V_{ee',e'} \zeta(\hbar\omega - E_{ee'}) \right\}. \quad (10)$$

This equation includes matrix elements of the operator \hat{V} of the interaction between atoms and electromagnetic field, $\zeta(x)$ is a singular function which is determined by the relation $\zeta(x) = \lim_{k \rightarrow \infty} (1 - \exp(ikx))/x$. To calculate the Green's matrix, we should perform a summation over resonant single-photon states "g" as well as over nonresonant states with two excited atoms and one photon "ee" (as greater length, see Ref. [36]). Actually, this approach allows one to describe from a single position both monatomic dynamics and cooperative effects caused by interatomic dipole-dipole interaction. The main idea of this approach was proposed by Foldy [37], further it was developed by a number of authors, to name a few [38–42]. This method was successfully used in our group for the analysis of the optical properties of dense atomic ensembles as well as for studying light scattering from such ensembles [43–49]. Further it allowed us to describe cooperative effects in atomic ensembles located in a Fabry-Perot cavity [28,29] and near a conducting surface [50–52].

The explicit expressions for the elements of the Green's matrix corresponding to a waveguide were derived in [32] (see, mainly, the Appendix in Ref. [32]).

By the inverse Fourier transform, we get the dynamics of the quantum amplitudes in a time domain, $b_e(t)$:

$$b_e(t) = \int_{-\infty}^{\infty} \frac{id\omega}{2\pi} \times \frac{b_s \exp(-i\omega t) \sum_{e' \neq s} R_{ee'}(\omega) \Sigma_{e's}(\omega)}{\omega - \omega_s - \Sigma_s(\omega)}, \quad (11)$$

where

$$\Sigma_s(\omega) = -i\frac{\gamma_s}{2} + \sum_{e, e' \neq s} \Sigma_{se}(\omega) R_{ee'}(\omega) \Sigma_{e's}(\omega). \quad (12)$$

Further, we go to the stationary limit of atomic excitation by an external unaffected light source. For this, we should remove the reverse influence of the atomic ensemble on the source atom and then consider $\gamma_s \rightarrow 0$ and $t \rightarrow \infty$ assuming $\gamma_s t \ll 1$. Technically, it can be performed as follows. Firstly, it is important to clarify the physical sense of Eq. (12). Here, the first term describes self-action of the source atom, and second term describes the influence of atoms forming an ensemble on the source atom. Thus, in order to simulate unaffected light source from the considered source-atom, we should artificially eliminate the second term in Eq. (12). After that, we go to the limit $\gamma_s \rightarrow 0$, which means monochromatic probe light. Looking at the denominator in Eq. (11), we can write

$$\lim_{\gamma_s \rightarrow 0} \frac{1}{\omega - \omega_s + i\frac{\gamma_s}{2}} = \zeta(\omega - \omega_s),$$

where $\zeta(x)$ is a singular function. Next, we go to the limit $t \rightarrow \infty$, which describes the stationary regime. Here, we can use the relation

$$\lim_{t \rightarrow \infty} \zeta(\omega - \omega_s) \exp(-i\omega t) = -2\pi i \delta(\omega - \omega_s) \exp(-i\omega_s t).$$

Useful relations between singular functions, which underlie these calculations, can be found in the textbook, Ref. [53]. Thus, after these limiting passages, we obtain the final expression:

$$b_e(t) = \exp(-i\omega_s t) \sum_{e' \neq s} R_{ee'}(\omega_s) \Sigma_{e's}(\omega_s), \quad (13)$$

where $R_{ee'}(\omega)$ is a resolvent operator of the considered multiatomic ensemble, which is defined as $R_{ee'}(\omega) = [(\omega - \omega_0)\delta_{ee'} - \Sigma_{ee'}(\omega)]^{-1}$.

Since the photodetector measures the electric component of the electromagnetic field, namely, $\overline{\mathbf{E}^{(-)}\mathbf{E}^{(+)}}$, we define the transmission coefficient as follows: $T = P_t/(P_t + P_r)$, where P_t is the total power of the electric component in the transmitted light and P_r refers to the same quantity in the reflected radiation. Both P_t and P_r can be naturally calculated as corresponding intensities integrated over the whole area of cross section of a waveguide.

The electric component of the light intensity can be calculated in a straightforward manner, as it was done in Refs. [49,54], or it can be simulated on the basis of the alternative method, which considers the so-called "atom detector". The idea of this alternative approach is taking into consideration an imaginary elusive "atom", which sense radiation emitted by the environment medium but do not re-emit photons. So, it works as a point detector. It is also important here that atom detector must perceive any kind of polarization of electromagnetic waves with equal susceptibility. The intensity of light at the point of the atom detector is proportional to its excited state population. Thus, the calculation of the transmission coefficient, T , is reduced to the calculation of the population of the excited state of the atom detector in two cases: when the atom detector is behind the atomic ensemble to get P_t and before the medium to get P_r . In the last case, we

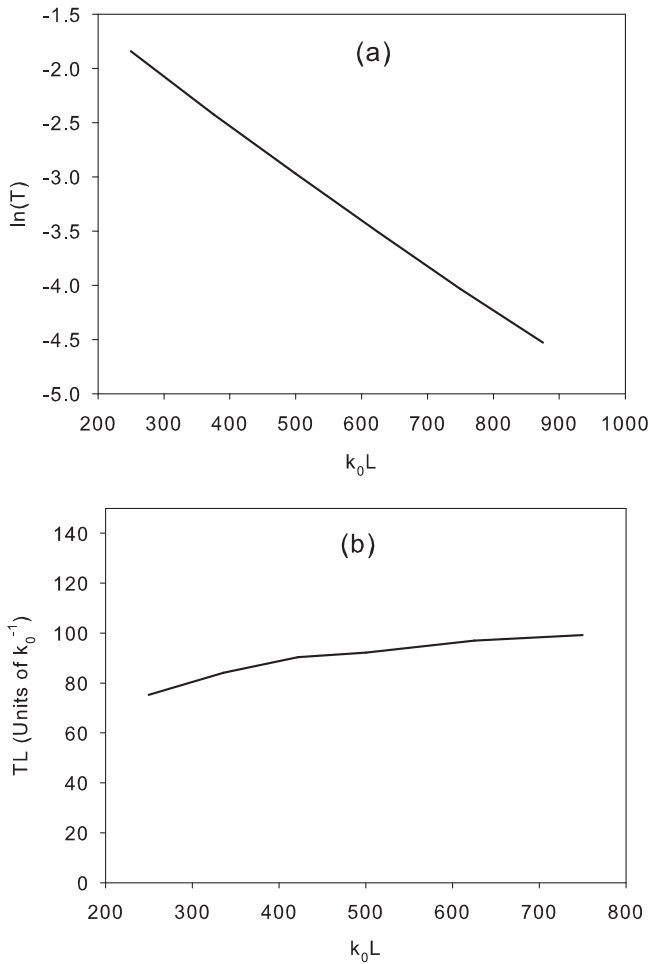


FIG. 2. Transmission depending on the length of atomic medium in a waveguide. $n = 2 \times 10^{-3}$, $\Delta = \gamma_0$. (a) $a = 4$, $b = 2$; (b) $a = b = 8$.

artificially exclude the primary radiation produced directly by the laser source from the consideration.

III. RESULTS AND DISCUSSION

Figure 2 shows the transmission coefficient depending on the length of atomic sample, $T(L)$, for both cases of a single-mode waveguide, Fig. 2(a), and a multimode one, Fig. 2(b). The transverse sizes of a waveguide were chosen as $a = 4$, $b = 2$ when plotting Fig. 2(a) and $a = b = 8$ when plotting Fig. 2(b). $1/k_0 = c/\omega_0$ defines a unit of length. The mode composition of a waveguide can be easily justified on the basis of well-known expression for cutoff frequencies of different modes, $\omega_c = c\sqrt{(m\pi/a)^2 + (n\pi/b)^2}$, where m and n are transverse indexes of a given mode. Thus, in the case of $a = 4$, $b = 2$, only the TE_{10} mode can propagate in a waveguide at long distances as an oscillating wave at the transition frequency, while in the case of $a = b = 8$, there are 10 such modes: TE_{10} , TE_{01} , TE_{20} , TE_{02} , TE_{11} , TE_{12} , TE_{21} , TM_{11} , TM_{12} , TM_{21} .

Atomic density is chosen sufficiently small, $n = 2 \times 10^{-3}$, so that cooperative effects in free space are negligible and, *a fortiori*, Anderson localization of light in free space ensemble is impossible. The detuning of the probe frequency related to

the resonant frequency of atomic transition, $\Delta = \omega_s - \omega_0$, is chosen $\Delta = \gamma_0$. Under a given condition, the mean free path of a photon can be estimated on the basis of its free space value,

$$l_{ph} = \frac{1}{n\sigma_0} \times \frac{\Delta^2 + (\gamma_0/2)^2}{(\gamma_0/2)^2}, \quad (14)$$

where σ_0 is single-atom resonant cross section, $\sigma_0 = 6\pi$. Substituting the given values of n and Δ in Eq. (14), we get $l_{ph} \approx 133$. So, in order to study incoherent light transfer, we should consider the values of L several times larger than this estimation. That is exactly we do when plotting Fig. 2.

Figure 2(a) shows that in a single-mode waveguide, the dependence $T(L)$ is exponential, $T(L) = T_0 \exp(-L/l_{loc})$. This indicates on the regime of Anderson localization of light, the parameter l_{loc} means the localization length and T_0 is normalization parameter. For given parameters, $T_0 \approx 0.43$ and $l_{loc} \approx 235$. With increasing in the transverse sizes of a waveguide, a and b , both parameters T_0 and l_{loc} undergo complex steplike changes. Sharp steps correspond to the changes in the mode composition of a waveguide, e.g., when single-mode waveguide turns out to be two-mode. With further increasing in the transverse sizes, the nature of transmittance scaling itself changes and ceases to be purely exponential. Thus, in the case of the multimode waveguide, the dependence $T(L)$ becomes close to hyperbolic, $T(L) \propto 1/L$, see Fig. 2(b). This indicates on the regime of classical diffuse radiation transfer.

It can be also useful to plot the dependencies $T(L)$ for the intermediate cases of the few-mode waveguide. Figure 3 demonstrates this behavior for the case $a = b = 4$ (two-mode waveguide, TE_{10} and TE_{01} modes are present) and for the case $a = b = 5$ (four-mode waveguide, TE_{11} and TM_{11} modes add to the previous ones). For clarity, we show $\ln(T)$ in Fig. 3(a) as well as TL in Fig. 3(b). It is hardly to identify the character of the dependence $T(L)$ for a few-mode waveguide definitely. In our glance, for the two-mode case, it is closer to exponential law; whereas for the four-mode case, it is closer to the hyperbolic one.

In addition, we have investigated the dependence of the transmission coefficient on the transverse size of a waveguide when the length of atomic medium is fixed, see Fig. 4. The cross section of a waveguide is square, so $a = b$. In Fig. 4, we observe complicated nonmonotonic behavior with extremely sharp changes in the vicinities of the critical values of the transverse size which correspond to the changes in the mode composition of a waveguide (indicated by reference dashed lines). We do not smooth the curve in order to better demonstrate the difference in the gradient for vicinities of the critical values of the transverse size and for the areas far from these critical points.

The effect shown in Fig. 4 is much unexpected. In our opinion, its qualitative explanation is connected with multiple interference between different modes of the electromagnetic field. It is especially important in the cases when the transverse size of a waveguide, a , is close to the critical values indicated by vertical dashed lines, because in the right side of their vicinities we get new allowed modes with small z projection of the wave vector. For these modes, interference phenomena are especially important, because a photon undergoes a huge number of reflections from the walls of a

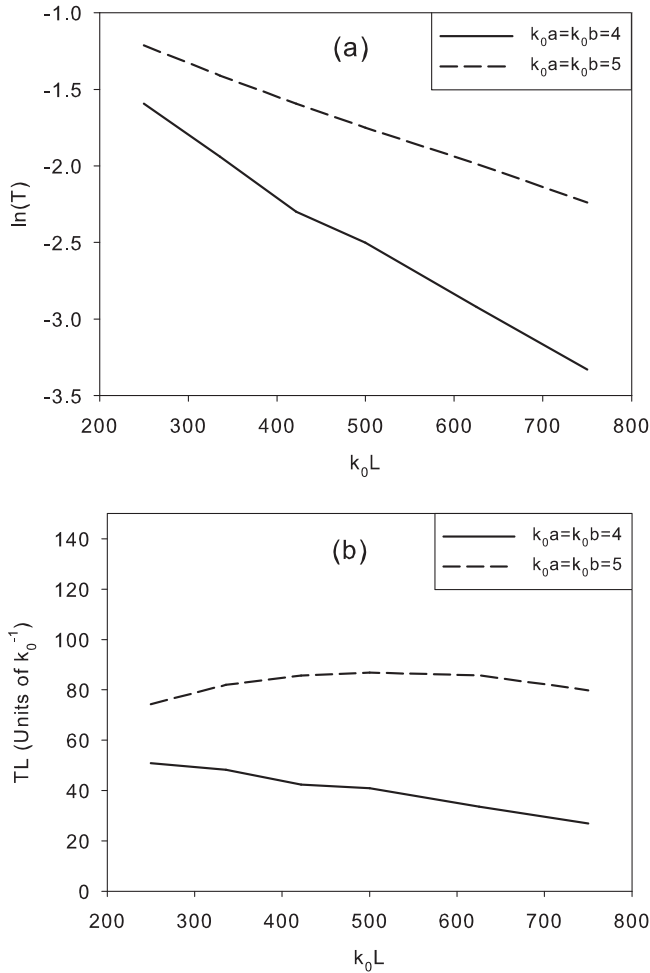


FIG. 3. Transmission depending on the length of atomic medium in a waveguide. Solid curves refer to the case of two-mode waveguide with sizes $a = b = 4$; dashed curves correspond to the four-mode case when $a = b = 5$. Other parameters are the same as in Fig. 2.

waveguide. This interference can be constructive or destructive depending on a number of parameters; as a result we observe the enhancement of transmission, e.g., near the critical points $a = \pi\sqrt{2}$ and $a = 2\pi$, or its suppression, like in the right side of the vicinity of critical point $a = \pi\sqrt{5}$.

IV. CONCLUSION

In conclusion, we have calculated the transmission of disordered atomic ensemble in a waveguide on the basis of self-consistent quantum microscopic treatment taking into account 3D arrangement of atoms and the vectorial nature of the electromagnetic field. We have found that the nature of light transport essentially depends on the transverse sizes of a waveguide. A single-mode waveguide with small transverse

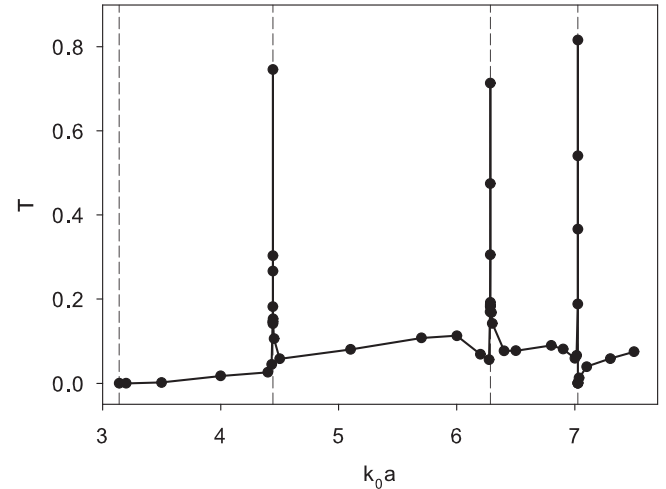


FIG. 4. The dependence of the transmission coefficient on the transverse size of a waveguide with square cross section, $a = b$. $L = 1000$, other parameters are the same as in Fig. 2. Vertical dashed lines indicate critical values of the transverse size when new modes appear: $\pi\sqrt{2}$ (permitting TE_{11} and TM_{11} modes); 2π (permitting TE_{20} and TE_{02} modes); $\pi\sqrt{5}$ (permitting TE_{12} , TE_{21} , TM_{12} , TM_{21} modes). Leftmost vertical dashed line indicates the minimal value of the transverse size, π , which corresponds to the cutoff. The curve is not smoothed, calculated points are indicated by circles.

sizes exhibits Anderson localization of light, which manifests itself in exponential decrease of the transmittance with increasing in the thickness of atomic sample. An increase of the transverse sizes breaks exponential law, so that in a few-mode waveguide we observe complicated dependence of the transmission on the thickness due to complex interplay between Anderson localization of light and diffuse radiation transfer. With further increasing of the transverse sizes of a waveguide, the transmission scaling obeys hyperbolic law, which indicates on the regime of diffuse transfer in a multi-mode waveguide.

Finally, we would like to note that light localization is a rather general phenomena, taking place in a wide range of physical systems. In the present paper, we discussed conventional Anderson localization of light induced by disorder. However, light localization can be obtained in different ways besides Anderson scheme. One of examples is described in Ref. [55], where the authors analyze a coherence-driven photonic nanosystem in the nonequilibrium configuration.

ACKNOWLEDGMENTS

This work was supported by the Russian Science Foundation (Grant No. 21-72-10004). The results of the work were obtained using computational resources of Peter the Great St. Petersburg Polytechnic University Supercomputer Center.

[1] P. W. Anderson, *Phys. Rev.* **109**, 1492 (1958).
 [2] J. Chabe, G. Lemarie, B. Gremaud, D. Delande, P. Szriftgiser, and J.-C. Garreau, *Phys. Rev. Lett.* **101**, 255702 (2008).

[3] F. Jendrzejewski, A. Bernard, K. Muller, P. Cheinet, V. Josse, M. Piraud, L. Pezze, L. Sanchez-Palencia, A. Aspect, and P. Bouyer, *Nat. Phys.* **8**, 398 (2012).

- [4] D. S. Wiersma, P. Bartolini, A. Lagendijk, and R. Righini, *Nature (London)* **390**, 671 (1997).
- [5] M. Storzer, P. Gross, C. M. Aegerter, and G. Maret, *Phys. Rev. Lett.* **96**, 063904 (2006).
- [6] T. Sperling, W. Buhner, C. M. Aegerter, and G. Maret, *Nat. Photonics* **7**, 48 (2013).
- [7] H. Hu, A. Strybulevych, J. H. Page, S. E. Skipetrov, and B. A. van Tiggelen, *Nat. Phys.* **4**, 945 (2008).
- [8] A. Aubry, L. A. Cobus, S. E. Skipetrov, B. A. van Tiggelen, A. Derode, and J. H. Page, *Phys. Rev. Lett.* **112**, 043903 (2014).
- [9] L. Sapienza, H. Thyrrestrup, S. Stobbe, P. D. Garcia, S. Smolka, and P. Lodahl, *Science* **327**, 1352 (2010).
- [10] J. Liu, P. D. Garcia, S. Ek, N. Gregersen, T. Suhr, M. Schubert, J. Mork, S. Stobbe, and P. Lodahl, *Nat. Nanotechnol.* **9**, 285 (2014).
- [11] F. Pratesi, M. Burrese, F. Riboli, K. Vynck, and D. S. Wiersma, *Opt. Express* **21**, A460 (2013).
- [12] F. Scheffold, R. Lenke, R. Tweer, and G. Maret, *Nature (London)* **398**, 206 (1999).
- [13] T. van der Beek, P. Barthelemy, P. M. Johnson, D. S. Wiersma, and A. Lagendijk, *Phys. Rev. B* **85**, 115401 (2012).
- [14] F. Scheffold and D. Wiersma, *Nat. Photonics* **7**, 934 (2013).
- [15] S. E. Skipetrov and I. M. Sokolov, *Phys. Rev. Lett.* **112**, 023905 (2014).
- [16] S. E. Skipetrov and I. M. Sokolov, *Phys. Rev. Lett.* **114**, 053902 (2015).
- [17] D. E. Chang, J. S. Douglas, A. Gonzalez-Tudela, C.-L. Hung, and H. J. Kimble, *Rev. Mod. Phys.* **90**, 031002 (2018).
- [18] E. Abrahams, P. W. Anderson, D. C. Licciardello, and T. V. Ramakrishnan, *Phys. Rev. Lett.* **42**, 673 (1979).
- [19] F. Evers and A. D. Mirlin, *Rev. Mod. Phys.* **80**, 1355 (2008).
- [20] A. Goban, K. S. Choi, D. J. Alton, D. Ding, C. Lacroute, M. Pototschnig, T. Thiele, N. P. Stern, and H. J. Kimble, *Phys. Rev. Lett.* **109**, 033603 (2012).
- [21] S.-P. Yu, J. D. Hood, J. A. Muniz, M. J. Martin, R. Norte, C.-L. Hung, S. M. Meenehan, J. D. Cohen, O. Painter, and H. J. Kimble, *Appl. Phys. Lett.* **104**, 111103 (2014).
- [22] T. Kobayashi, Q. Zheng, and T. Sekiguchi, *Phys. Rev. A* **52**, 2835 (1995).
- [23] E. V. Goldstein and P. Meystre, *Phys. Rev. A* **56**, 5135 (1997).
- [24] G. S. Agarwal and S. Dutta Gupta, *Phys. Rev. A* **57**, 667 (1998).
- [25] R. Rohlsberger, K. Schlage, B. Sahoo, S. Couet, and R. Ruffer, *Science* **328**, 1248 (2010).
- [26] Y.-Q. Zhang, L. Tan, and P. Barker, *Phys. Rev. A* **89**, 043838 (2014).
- [27] A. Goban, C.-L. Hung, J. D. Hood, S.-P. Yu, J. A. Muniz, O. Painter, and H. J. Kimble, *Phys. Rev. Lett.* **115**, 063601 (2015).
- [28] A. S. Kuraptsev and I. M. Sokolov, *J. Exp. Theor. Phys.* **123**, 237 (2016).
- [29] A. S. Kuraptsev and I. M. Sokolov, *Phys. Rev. A* **94**, 022511 (2016).
- [30] M. D. Lee, S. D. Jenkins, Y. Bronstein, and J. Ruostekoski, *Phys. Rev. A* **96**, 023855 (2017).
- [31] T. Botzung, D. Hagenmüller, S. Schütz, J. Dubail, G. Pupillo, and J. Schachenmayer, *Phys. Rev. B* **102**, 144202 (2020).
- [32] A. S. Kuraptsev and I. M. Sokolov, *Phys. Rev. A* **101**, 053852 (2020).
- [33] O. Morice, Y. Castin, and J. Dalibard, *Phys. Rev. A* **51**, 3896 (1995).
- [34] J. D. Jackson, *Classical Electrodynamics* (Wiley, New York, 1962).
- [35] W. R. Raudorf, *Am. J. Phys.* **46**, 35 (1978).
- [36] I. M. Sokolov, D. V. Kupriyanov, and M. D. Havey, *J. Exp. Theor. Phys.* **112**, 246 (2011).
- [37] L. L. Foldy, *Phys. Rev.* **67**, 107 (1945).
- [38] M. J. Stephen, *J. Chem. Phys.* **40**, 669 (1964).
- [39] D. A. Hutchinson and H. F. Hameka, *J. Chem. Phys.* **41**, 2006 (1964).
- [40] R. Bonifacio, P. Schwendimann, and F. Haake, *Phys. Rev. A* **4**, 302 (1971).
- [41] R. Bonifacio, P. Schwendimann, and F. Haake, *Phys. Rev. A* **4**, 854 (1971).
- [42] Z. Ficek, R. Tanas, and S. Kielich, *Optica Acta* **33**, 1149 (1986).
- [43] Ya. A. Fofanov, A. S. Kuraptsev, I. M. Sokolov, and M. D. Havey, *Phys. Rev. A* **84**, 053811 (2011).
- [44] I. M. Sokolov, A. S. Kuraptsev, D. V. Kupriyanov, M. D. Havey, and S. Balik, *J. Mod. Opt.* **60**, 50 (2013).
- [45] A. S. Kuraptsev and I. M. Sokolov, *Phys. Rev. A* **91**, 053822 (2015).
- [46] S. Roof, K. Kemp, M. Havey, I. M. Sokolov, and D. V. Kupriyanov, *Opt. Lett.* **40**, 1137 (2015).
- [47] S. E. Skipetrov, I. M. Sokolov, and M. D. Havey, *Phys. Rev. A* **94**, 013825 (2016).
- [48] A. S. Kuraptsev and I. M. Sokolov, *Laser Phys.* **27**, 115201 (2017).
- [49] A. S. Kuraptsev, I. M. Sokolov, and M. D. Havey, *Phys. Rev. A* **96**, 023830 (2017).
- [50] A. S. Kuraptsev and I. M. Sokolov, *JETP* **127**, 455 (2018).
- [51] A. S. Kuraptsev and I. M. Sokolov, *Laser Phys.* **28**, 085203 (2018).
- [52] A. S. Kuraptsev and I. M. Sokolov, *Phys. Rev. A* **100**, 063836 (2019).
- [53] W. Heitler, *The Quantum Theory of Radiation* (Oxford University Press, London, 1954).
- [54] I. M. Sokolov, *Laser Phys.* **25**, 065202 (2015).
- [55] K. L. Tsakmakidis, P. K. Jha, Y. Wang, and X. Zhang, *Sci. Adv.* **4**, eaaq0465 (2018).